

# Design of a 2-Finger Hand Exoskeleton for VR Grasping Simulation

Panagiotis Stergiopoulos, Philippe Fuchs and Claude Lurgeau

Robotics Center-Ecole des Mines de Paris  
60 bd St-Michel, 75272 Paris Cedex 06, France  
e-mail: [panagiotis.stergiopoulos@ensmp.fr](mailto:panagiotis.stergiopoulos@ensmp.fr)

**Abstract.** There are numerous applications of VR simulation requiring the grasping and manipulation of virtual objects. Standard-use haptic interfaces (e.g. Virtuose 6D, PHANTOM) allow only a limited level of realism, as grasping is approximated through a metaphor (e.g. pressing a button for grasping an object). Existing hand exoskeletons have also certain drawbacks (e.g. feedback only for finger flexion, limited finger workspace etc.). The work presented in this paper introduces a hand force exoskeleton that allows full finger flexion and extension and applies bi-directional feedback. It has 3dof at the index finger and 4 at the thumb. The system is actuated by DC motors and cable transmissions are used. It has been designed for use in conjunction with Virtuose 6D, a commercial 6dof haptic arm, in order to allow the simulation of external forces (gravity, contact reaction forces, etc.).

## 1 Introduction

As the field of haptics evolves, the application of force feedback techniques in VR become more demanding. Such VR applications include now simulations of medical operations, assembling of mechanism parts or evaluation of ergonomics (e.g. of car or other vehicle dashboards).

There are two important issues for achieving a good level of realism. The first issue is the sufficiency of the available software. One of the more important shortcomings of this form is the speed of the collision detection algorithms and the modeling of interactions between the user and the Virtual Environment (VE). There are however some recent algorithms that may give a satisfactory solution to the simulation of interaction between virtual objects (they mostly apply to rigid objects).

The second important issue is the adequacy of current interfaces. We can already separate them into 2 main categories, a) the general-purpose interfaces that allow mostly the interaction with the VE through a tool [4], [11], and b) the interfaces that allow the use of the user's fingers. The interfaces of the first category can give good results when there is indirect contact with a virtual object. When however the task

demands dexterous actions, they are less realistic. They usually approximate real tasks through a metaphor (e.g. grasping of an object with the fingers is substituted by pressing a certain button on the interface tool, when in contact with the object). In certain cases, such as the studies of ergonomics, these metaphors cannot be accepted, as the evaluation of the virtual action requires the accurate simulation of the real one.

Already some interfaces provide the possibility of simulating grasping. The CyberGrasp is such a system, which, through a system of tendons, applies forces at the fingertip of each of the 5 fingers and resists their flexion, [6]. The long cable sheaths increase however friction, while due to the contact of the exoskeleton with the back part of each finger, the user can feel “ghost forces” on the whole finger, even when they should be limited on the fingertip, [12]. The other disadvantage is that the exoskeleton can resist only the flexion but not the extension of the fingers. CyberGrasp used in conjunction with a haptic arm forms the CyberForce, which can also simulate the reaction force of the contact with a virtual object, the gravity etc.

The SARCOS exoskeleton was also used in experiments for the simulation of object grasping, [9]. This exoskeleton can apply feedback to the arm and 2 fingers and its weight (although important) is compensated by its hydraulic actuators. The inertial forces however continue to be felt by the user.

The Rutgers Master II provides feedback at the fingertips of 4 fingers (no feedback for the small finger) by connecting on each of them a mini pneumatic piston, [1]. This interface is very light, but the positioning of the actuators in the palm of the user limits by an important factor the possible flexion of each finger.

Choi *et al* have introduced an exoskeleton for two fingers that can apply bi-directional forces on each phalange, [3]. They have chosen the use of ultrasonic motors for their high power-to-weight ratio.

Researchers of the University of Wisconsin have also presented a 1-finger prototype of a mechanism that allows full finger flexion and extension and they analyze the haptic effect perceived by the user, [12]. They take into account only one variable of the finger flexion for modeling and controlling the finger movement.

More recently, a new 3-finger exoskeleton was presented by researchers of Keio University, [7]. It provides 4dof per finger and it uses a combination of clutches and elastic elements for applying passive force feedback to the fingers.

Finally, the PERCRO laboratory of the Scuola Superiore Sant’Anna introduced the design of a hand haptic device that would apply force feedback to two fingers, while positioning the actuators on the forearm, [5]. This would be achieved by linking the fingers to the motors through a serial mechanism for each finger.

In this paper, we present a 2-finger haptic interface that offers feedback for both finger flexion and extension and also allows the exploitation of the whole hand flexion workspace. It can be adapted to most hand sizes. The DC motors are fixed on the exoskeleton and cable transmissions are used for actuating the fingers. It will be used with the Virtuoso 6D haptic device, for allowing the simulation of object grasping and the simultaneous application of external and internal forces. The first application is the ergonomics studies of the dashboard of a car.

## 2 Concept

The human hand is probably the most difficult system to emulate with a robotic mechanism and this difficulty applies also to the design of exoskeletons for the hand. The major problems are the very high number of degrees of freedom (4 major ones per finger, which are sometimes coupled with less important movements) and the variety of hand sizes. For example, the flexion/extension of the thumb is combined with a rotation of the thumb phalanges around their axis, an action that is called opposition. Even though it could be possible to make a system that imitates this combination for a specific hand, it is not easy to make it for all hand sizes. It is thus necessary to choose which of the degrees of freedom of the hand are important in VR applications. We can separate the tasks executed with our hand in 3 categories:

1. Tasks that require the use of only one finger. Such examples are feeling the surface of an object, pressing a button etc.
2. Tasks that require the pulling of levers, pushing objects etc. Examples are the use of a gearbox or the handbrake and they can be done either with a minimum of 2 fingers or with the thumb and the rest of the fingers working together.
3. Tasks that require dexterous manipulations. Such tasks are holding an object with the fingers, turning a radio button etc. They demand the simultaneous use of at least 3 fingers (turning a button can be done with 2 fingers, but it's sometimes more practical with 3).

In our case we have chosen to use 2 fingers as the principal application of our interface is the ergonomics evaluation of a car dashboard. Our primary objectives are the appreciation of the accessibility of the instruments in a car and the practicability of using them. As we don't need to pick up any object, a system using only 2 fingers suffices for the initial study of the task. We are planning however to develop a 3-finger interface in the future for realizing more complicated tasks. As we also need to simulate the effect of external forces (e.g. forces of interaction when pushing or pulling an object etc.), we will couple the hand exoskeleton with a grounded haptic device that will provide this force feedback. Our choice is the Virtuose 6D, a commercial haptic device with 6 actuated dof that can apply significant forces (>30N) and torques (~3Nm).

In order to choose the actuators of the exoskeleton, we have used a force sensor (Fig. 1), for measuring the force capacity of the hand. The results are presented in Table 1. They don't represent average values given for an ideally large mixed group of the population, but they give an indication of the necessary force range.

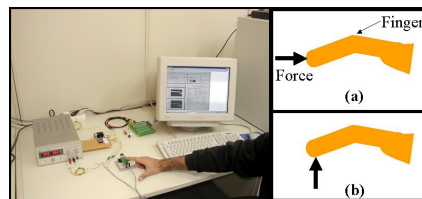


**Fig. 1.** Finger force measurement for forces a) in the direction of the phalange axis and b) perpendicular to it

These values are given for forces applied at the fingertip and while only one finger was used at a time (the simultaneous use of 2 or more fingers further raises the force capacity). We must notice that the aforementioned values are not usually applied in practice, as we use such force on the fingers only in actions of great strain (e.g. pushing or lifting a heavy object), so we could choose our actuators for considerably smaller forces depending on the application. In our case, the scope of the exoskeleton is to permit the exploring of surfaces with the hand and the manipulation of small devices, such as buttons. Although for some buttons the maximum force can be higher than 20N, its application is instantaneous and so the actuators could be chosen for applying only instantaneously forces of this magnitude.

**Table 1.** Finger force capacity (forces applied at the fingertip)

Finger	Continuous maximum force perpendicular to the fingertip (N)	Continuous maximum force in the direction of the phalange (N)
Thumb	15	35
Index	10	32
Middle	10	30
Ring	9	24
Pinkie	8	18

### 3 Interface Design

#### 3.1 Mechanism Kinematics

One of our objectives is to control the finger movements for both flexion and extension and with a minimum of actuators (diminishing mechanism complexity and weight at the same time). We have thus chosen the use of a 3-link serial mechanism for controlling the finger movements (the third link has zero length it's in fact limited to a point, the last joint, Fig. 2b). This mechanical structure has the advantage of allowing full finger flexion and extension. The alternative solution of having a 3 bar structure for each phalange demands the independent control of the flexion of each phalange (Fig. 2a). This solution would also allow the user to feel forces on each phalange, whereas the solution we choose is applying forces only at the fingertips. This poses no problem, as we manipulate objects mostly with the fingertips (whereas using a power grasp for pulling levers doesn't demand precise force feedback on the whole finger).

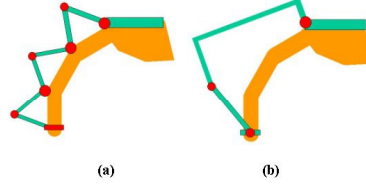


Fig. 2. Mechanisms for a) independent phalange control b) fingertip control

The current version of the interface has 7dof for the hand, 3 for the index finger (all the flexions) and 4 for the thumb (all the flexions plus the adduction). One degree of freedom is actuated per finger, i.e. the base flexion. Our system applies bi-directional forces, permitting thus to have a haptic feeling on the finger even when we extend them (contrary to interfaces that used cables attached on the back of the fingertips). Although it is possible to use 2 or three motors per finger in the future, an under-actuated scheme was chosen in order to reduce the weight. The disadvantage in this case is that the direction of the applied force on the fingertip is affected by the relative orientation of the finger. This is partially counterbalanced by the haptic arm, which applies a correctly directed force on the top of the hand (Fig. 3). Thus, although forces applied in a restricted way on the fingers, the combined feedback of the exoskeleton and the haptic arm can create a convincing illusion (as in the CyberForce when it applies forces at the back of the fingers).

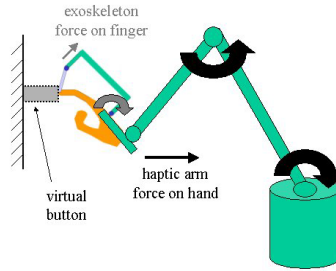


Fig. 3. Cooperation of haptic arm/exoskeleton

The differential kinematics for the finger mechanism (for the finger flexion) are given by Equation 1:

$$\begin{bmatrix} \dot{x} \\ \dot{y} \\ \omega_z \end{bmatrix} = \begin{bmatrix} -l_1 \cdot s_1 - l_2 \cdot s_{12} - l_3 \cdot s_{123} & -l_2 \cdot s_{12} - l_3 \cdot s_{123} & -l_3 \cdot s_{123} \\ l_1 \cdot c_1 + l_2 \cdot c_{12} + l_3 \cdot c_{123} & l_2 \cdot c_{12} + l_3 \cdot c_{123} & l_3 \cdot c_{123} \\ 1 & 1 & 1 \end{bmatrix} \cdot \begin{bmatrix} \dot{q}_1 \\ \dot{q}_2 \\ \dot{q}_3 \end{bmatrix} \quad (1)$$

As the 3<sup>rd</sup> link has zero length, the equation is reduced to:

$$\begin{bmatrix} \dot{x} \\ \dot{y} \\ \omega_z \end{bmatrix} = \begin{bmatrix} -l_1 \cdot s_1 - l_2 \cdot s_{12} & -l_2 \cdot s_{12} & 0 \\ l_1 \cdot c_1 + l_2 \cdot c_{12} & l_2 \cdot c_{12} & 0 \\ 1 & 1 & 1 \end{bmatrix} \begin{bmatrix} \dot{q}_1 \\ \dot{q}_2 \\ \dot{q}_3 \end{bmatrix} \quad (2)$$

The corresponding equations for the finger flexion are:

$$\begin{bmatrix} \dot{x} \\ \dot{y} \\ \omega_z \end{bmatrix} = \begin{bmatrix} -l_{PP} \cdot s_{\theta_1} - l_{MP} \cdot s_{\theta_{12}} - l_{DP} \cdot s_{\theta_{123}} & -l_{MP} \cdot s_{\theta_{12}} - l_{DP} \cdot s_{\theta_{123}} & -l_{DP} \cdot s_{\theta_{123}} \\ l_{PP} \cdot c_{\theta_1} + l_{MP} \cdot c_{\theta_{12}} + l_{DP} \cdot c_{\theta_{123}} & l_{MP} \cdot c_{\theta_{12}} + l_{DP} \cdot c_{\theta_{123}} & l_{DP} \cdot c_{\theta_{123}} \\ 1 & 1 & 1 \end{bmatrix} \begin{bmatrix} \dot{\theta}_1 \\ \dot{\theta}_2 \\ \dot{\theta}_3 \end{bmatrix} \quad (3)$$

where  $q_1, q_2, q_3$  are the angles of rotation of the three joints of the mechanism,  $\theta_1, \theta_2, \theta_3$  are the rotations of the finger phalanges,  $s_1$  is the  $\sin()$  of angle  $q_1$ ,  $c_1$  is the  $\cos()$  of angle  $q_1$ ,  $c_{12}$  is the  $\cos()$  of  $q_1+q_2$ ,  $c_{\theta_{12}}$  is the  $\cos()$  of  $q_{\theta_1}+q_{\theta_2}$ ,  $l_1$  and  $l_2$  are the lengths of the first two links of the mechanism,  $l_{PP}$  is the length of the proximal phalange,  $l_{MP}$  is the length of the middle phalange and  $l_{DP}$  the one of the distal phalange. The 3-link mechanism becomes singular when  $q_2 = \pm\pi$  or  $0$ . For avoiding these values for the joint angles, we choose the length of the mechanism links so as to keep them out of its workspace. For achieving that, we accept in practice that for the full grasp position (Fig. 4), the angle  $q_1$  should be equal to  $q_{1gr}$  (we choose  $80^\circ$ ) and angle  $q_2$  should be  $q_{2gr}$  ( $150^\circ$ ). By applying these values, we get :

$$l_1 = \frac{(x_{gr} - l_H) s_{gr12} - (y_{gr} - l_N) c_{gr12}}{c_{gr1} s_{gr12} - s_{gr1} c_{gr12}} \quad (4)$$

$$l_2 = \frac{c_{gr1} (y_{gr} - l_N) - s_{gr1} (x_{gr} - l_H)}{c_{gr1} s_{gr12} - s_{gr1} c_{gr12}} \quad (5)$$

where coordinates  $x_{gr}$  and  $y_{gr}$  of the center of the fingertip in full grasping (measured with respect to the metacarpophalangeal joint for each user) and  $l_H$  and  $l_N$  is the horizontal and perpendicular distance respectively between the metacarpophalangeal (MCP) finger joint and the first joint (axis of rotation  $q_1$ ) of the mechanism.

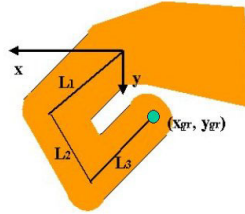


**Fig. 4.** Finger full grasp position

### 3.2 Transmission Choice

For placing the motors in a position that the haptic arm can easily compensate their weight, we have used cable transmissions. The problem that arises during the choice of the cable path is keeping the length of the cables constant for different finger orientation. There are two ways for placing the cable path:

1. Passing the cables from each axis of rotation that lies between the motor and the controlled joint.
2. Passing the cables in a way that the same length of cable that wraps around the pulley, is unwrapped around the other side of the pulley.

Examples of appropriate cable path choice have been given in [10]. We have chosen the second solution because it limits less the rotational workspace and the cables are less prone of slipping out of the pulleys than in the first one. The first solution also demands very high precision, otherwise the total cable length can change or they can slip out of the pulley.

This kind of transmission is necessary for passing the cables around the thumb adduction rotation axis, towards the thumb flexion rotation axis (Fig 5 and Fig. 6). By using two pulleys of the same radius, when the thumb rotates (adduction), as one part of the cable wraps around the first pulley and the dotted part unwraps around the second for the same degrees, the total length of the cable remains constant. A disadvantage of this solution is that the adduction and the flexion of the finger are coupled. This means that the thumb motor encoder is measuring simultaneously these two rotations. By comparing the results of the 2 corresponding encoders (thumb motor and first thumb flexion encoders), we can find out if there was only one or both of these rotations and we can calculate each individual one.

An additional problem is that the thumb base is adjustable for different hands, so the length of the cable should change. For overcoming it, we have introduced intermediate pulleys whose axis can translate and in this way we can adjust the cable for different configurations of the thumb base (Fig. 7).

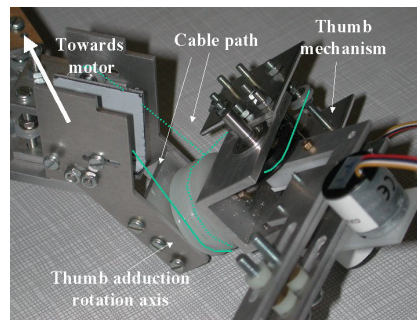


**Fig. 5.** Cable path around thumb adduction axis

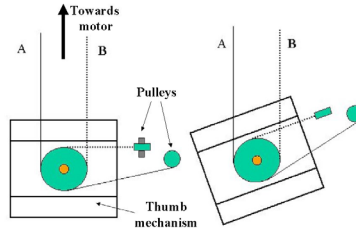


Fig. 6. Cable transmission for the thumb for constant cable length

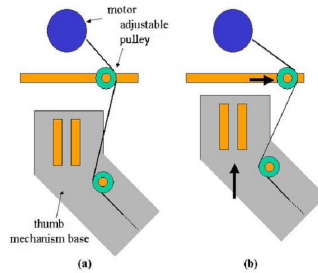


Fig. 7. Cable length adjustment for moving thumb base

The motors chosen are RE-max DC Maxon Motors with graphite brushes, because of their high torque/weight ratio. Another advantage is that the sampling rate of the encoders and the mechanical bandwidth of the motors allow rates of the haptic simulation loop of the order of one kHz, necessary for simulating rigid surfaces. It is very important to keep the weight of the motors as low as possible, fact that contradicts with the level of necessary output torque. For this reason we have used two solutions. The first is the use of a pulley transmission increasing the torque between the motor and the finger and the second is the use of a motor with planetary gears. The advantage of the first solution is the increase of output torque without an important increase in friction, while the use of gears is a more compact solution for increasing the torque. Nevertheless, the gears introduce backlash and higher friction. In order not to compromise the backdriveability of the mechanism, a low transmission ratio is chosen (5.4:1). Previous studies have shown that geared motors with even higher transmission rates could be used with haptic interfaces, [8].

### 3.2.1 Finger Angle Calculation

We measure the rotation of 5dof (out of 7) of the exoskeleton, 2 rotations through the encoders of the 2 motors plus 3 more through independent encoders. We are using 2 encoders per finger (an extra one is used for the adduction of the thumb), while each finger has 3 dof for flexion/extension. The flexion/extension of the proximal interphalangeal joint and distal interphalangeal joint are coupled for free hand movement, so there is a way to predict the orientation of each phalange by knowing the 2 encoder readings. The existence of trigonometric functions in the equations

leads to a 3x3 non-linear system that cannot be solved directly. Burdea et al propose the use of a pre-calculated table that correlates the 2 mechanism parameters to the phalanges' rotations [1]. Practice has however shown that with the right choice of parameters, an iterative method can quickly calculate the finger rotations. Considering that  $x_f$  and  $y_f$  are the coordinates of the fingertip on the plane of the finger flexion (Fig. 8), we calculate the distance of the fingertip from the MCP joint (Equation 6) and the angle of rotation of the fingertip with respect to the MCP joint (Equation 7):

$$R = \sqrt{(x_f)^2 + (y_f)^2} \quad (6)$$

$$\theta = \tan^{-1}\left(\frac{y_f}{x_f}\right) \quad (7)$$

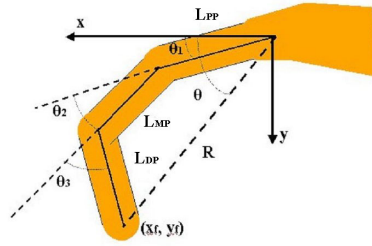


Fig. 8. Finger coordinates

Following that, we can notice that the three phalanges and the line connecting the fingertip to the finger base form a 4-bar structure, which has 1dof. Knowing that there is a relationship between the rotations  $\theta_2$  and  $\theta_3$  ( $\theta_3 = \theta_3(\theta_2)$ ), there is only one possible position for the structure. By applying the semitone theorem on the triangles EBC and EDA of Fig. 9 ( $0^\circ < \theta_2 + \theta_3 < 180^\circ$ ), we arrive to Equation 8, which is solved iteratively:

$$f(\theta_2) + g(\theta_2) - \theta_2 - \theta_3(\theta_2) = 0 \quad (8)$$

where:

$$f(\theta_2) = \sin^{-1}\left(\frac{L_{DP} + L_b}{R} \cdot \sin(\theta_2 + \theta_3(\theta_2))\right) \quad (9)$$

$$g(\theta_2) = \sin^{-1}\left(\frac{L_{PP} + L_a}{R} \cdot \sin(\theta_2 + \theta_3(\theta_2))\right) \quad (10)$$

$$L_a = \frac{\sin(\theta_3(\theta_2))}{\sin(\theta_2 + \theta_3(\theta_2))} \cdot L_{MP} \quad (11)$$

$$L_b = \frac{\sin(\theta_2)}{\sin(\theta_2 + \theta_3(\theta_2))} \cdot L_{MP} \quad (12)$$

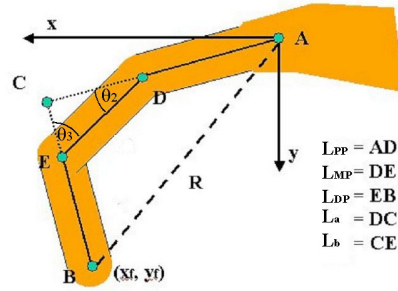


**Fig. 9.** Geometry for phalange orientation calculation

As initial value of the iterative method, we use the value of the angle  $\theta_2$  of the previous time step. As the angular displacement between iterations is very small (each iteration step is of the order of a ms), the algorithm converges rapidly to an acceptable approximation of the theoretical value (less than 0.01% difference most of the time). The time needed for this procedure is about  $5\mu\text{s}$  per finger and thus it doesn't affect the speed of the simulation.

The function  $\theta_3(\theta_2)$  gives the relationship between the 2 rotations. It is slightly different between fingers and persons and it is also affected by the possible application of force on the finger. For the free motion of the index finger the value proposed in [1] is:

$$\theta_3 = 0.46 \cdot \theta_2 + 0.083 \cdot \theta_2^2 \quad (13)$$

In practice, Equation 14 is giving a good approximation, considering the uncertainty about the exact position of the fingertip center for each individual user:

$$\theta_3 = 0.5 \cdot \theta_2 \quad (14)$$

When a force is applied, the relationship is affected as shown in Equation 15:

$$\theta_3 = 0.5 \cdot \theta_2 \mp K_N \cdot F_N \pm K_H \cdot F_H \quad (15)$$

where  $F_N$  is a force perpendicular to the fingertip,  $F_H$  is a force in the direction of the distal phalange. The parameters  $K_N$  and  $K_H$  differ between fingers and persons and Equation 15 just quantifies the effect of forces on the joint flexion.

It is obvious that for achieving great precision and correspondence between the movement of the real and the virtual fingers, we should: a) fix the mechanism on the hand in a way that does not allow any relative motion between the two of them (i.e.  $l_H$  and  $l_N$  are constant), and b) measure precisely the length of the phalanges of each finger. Practice has nevertheless shown that even without very precise calibration (important when many users should use the interface in a short period of time), the virtual finger follows realistically the movement of the real one.

#### 4 Mechanism Characteristics

Taking into account the transmission ratios, the position resolution is given in Table 2. The high resolution for the first flexion of each finger is the result of the high transmission ratio between each motor and actuated joint. Even the lowest achieved resolution is sufficient for general-purpose applications; it could nevertheless be further improved by using higher transmission ratios or more precise encoders (some have at least double resolution and almost half the weight, but their cost is quite higher). The current system gives (for an average finger of a length about 10cm) a fingertip movement resolution of about 0.5mm (depending on the finger size and orientation). In Table 2, we also present the maximum torque output for the two actuated joints.

**Table 2.** Mechanism position resolution

Mechanism joint	Resolution (degrees)	Maximum Torque (Nm)
Thumb, adduction	0.042°	-
Thumb, 3-bar, 1 <sup>st</sup> joint	0.36°	0.65
Thumb, 3-bar, 2 <sup>nd</sup> joint	0.36°	-
Index, 3-bar, 1 <sup>st</sup> joint	0.072°	0.28
Index, 3-bar, 2 <sup>nd</sup> joint	0.36°	-

The weight of the exoskeleton is considerable and it could cause fatigue to the user. For compensating this effect, we actively balance the weight of the exoskeleton with the haptic arm, by applying the appropriate current to each motor of the haptic arm. Equation 16 gives the relationship between the weight of the exoskeleton and the torque that should be applied by each actuator of the haptic arm:

$$T_m = J^T \cdot F_g \quad (16)$$

where  $T_m$  is the 6x1 vector of torques of each of the 6dof of the haptic arm,  $J^T$  is the transpose of the geometric Jacobian of the arm and  $F_g$  is the 6x1 vector of forces and torques applied at the center of gravity of the mechanism due to gravity. In order not to overestimate the torque for a joint due to identification errors (and as the center of gravity of the exoskeleton is slightly displaced when we move our fingers), we apply

only a fraction of each calculated torque. Otherwise, the compensating force may get greater than the weight of the exoskeleton and so inverting the gravitational force, effect that is more frustrating for the user.

Finally, for avoiding injuries due to too great or sudden forces, adjustable mechanical stops are used, limiting finger movement at the point of maximum extension.

## 5 Application

The described system (Fig. 10) is used in a simulation for the studies of ergonomics of car dashboards. The car interior is modeled with polygonal graphics and the virtual instruments can be programmed in order to simulate the behavior of real ones (e.g. by applying real force curves for push buttons, the handbrake etc.). The user interacts with the environment through a virtual representation of his hand and the forces between the hand and the virtual objects are calculated in a realistic way [13].

The simulation environment is going to be evaluated by ergonomics engineers, in order to consider if it could eventually replace the early stages of design and evaluation of a car dashboard.

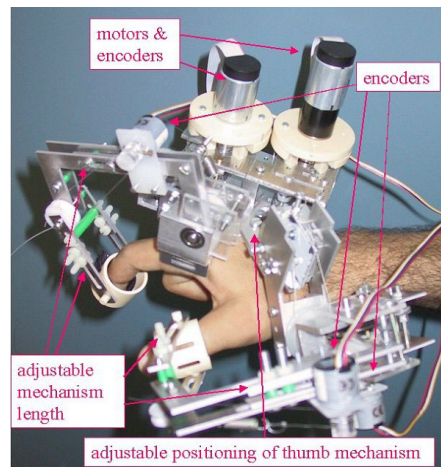


Fig. 10. 2-finger haptic interface

## 6 Conclusions and Future Work

We have presented a new haptic exoskeleton for the hand, designed for the simulation of touching and grasping objects with 2 fingers (thumb and index) in a Virtual Environment. The first version controls two fingers and it allows their full flexion and extension (plus adduction/abduction for the thumb). Unlike many other interfaces, it can apply forces that resist both the flexion and extension of the finger and the use of

DC motors allows a high bandwidth and force calculation update, which is necessary for stable simulation of textures and contact with rigid objects. The interface is going to be evaluated for the studies of ergonomics in the car manufacturing industry.

In the future, we consider ways of placing the motors of the exoskeleton further from the hand in order to make more comfortable to carry their weight. Another improvement is the eventual use of 3 fingers, as the simulation of dexterous manipulations would be rendered easier this way.

## 7 Acknowledgments

The work presented in this paper is a part of the research done for the PERF-RV Project, A5 Action, which is a subsidy of the French Ministry of Research and Technology. Its objective is the integration of force feedback in a VR simulation for the study of the ergonomics of vehicles. The first author was also supported by a Scholarship of the Alexander S. Onassis Public Benefit Foundation.

## References

1. Bouzit M., Popescu G., Burdea G., Boian R., "The Rutgers Master II-ND Force Feedback Glove", in the Proceedings of the VR2002 Haptics Symposium, Orlando FL, March 2002.
2. Burdea G., "Force and Touch Feedback for Virtual Reality", J. Wiley & sons inc., 1996.
3. Choi B. H., Choi H. R., "A Semi-direct Drive Hand Exoskeleton Using Ultrasonic Motor", in the Proceedings of the 1999 IEEE International Workshop on robot and Human Interaction, Pisa, Italy, September 1999, pp. 285-290. *Virtuose 6D*, Haption, <http://www.haption.com/>
4. Frisoli A., Simoncini F., Bergamasco M., "Mechanical Design of a Haptic Interface for the Hand", in the Proceedings of the ASME 2002 Design Engineering Technical Conferences and Computers and Information in Engineering Conference, Montreal, Canada, September 29-October 2, 2002.
5. Immersion 3D Interaction,
6. <http://www.immersion.com/products/3d/interaction/overview.shtml>
7. Koyama T., Yamano I., Takemura K., Maeno T., "Multi-fingered Exoskeleton Haptic Device Using Passive Force Feedback for Dexterous Teleoperation", in the Proceedings of 2002 IEEE/RSJ International Conference on Intelligent Robots and Systems", EPFL, Lausanne, Switzerland, October 2002, pp. 2905-2910.
8. Longnion J., Rosen J., Sinanan M., Hannaford B., "Effects of Geared Motor Characteristics on Tactile Perception of Tissue Stiffness", in the Studies in Health Technology and Informatics - Medicine Meets Virtual Reality, vol. 81, Newport Beach, CA, January 2001, pp. 286-292.
9. Maekawa H., Hollerbach J., "Haptic Display for Object Grasping and Manipulating in Virtual Environment", in the Proceedings of the 1998 International Conference of Robotics and Automation, Leuven, Belgium, May 1998, pp. 2566-2573.
10. Papadopoulos E., Vlachos K., Mitropoulos D., "On the Design of a Low-Force 5dof Force Feedback Haptic Mechanism", in Proceedings of the ASME 2002 Design Engineering Technical Conferences and Computers and Information in Engineering Conference, Montreal, Canada, September 29-October 2, 2002.
11. Phantom, Sensable Technologies Inc., [www.sensable.com](http://www.sensable.com)

12. Springer S., Ferrier N. J., “Design and Control of a Force-Reflecting Haptic Interface for Teleoperational Grasping”, in the Journal of Mechanical Design, June 2002, Vol. 124, pp. 277-283.
13. Stergiopoulos P., Moreau G., Ammi M., Fuchs P., “A Framework for the Haptic Rendering of the Human Hand”, in the Proceedings of the IEEE VR2003, 11th Symposium on Haptic Interfaces for Virtual Environments and Teleoperator Systems, Los Angeles CA, March 2003.